

**Surface Methane Concentrations Along the Mid-Atlantic Bight Driven by Aerobic
Subsurface Production Rather Than Seafloor Gas Seeps**

Mihai Leonte¹, Carolyn D. Ruppel², Angel Ruiz-Angulo³, and John D. Kessler¹

¹Department of Earth and Environmental Sciences, University of Rochester, Rochester, NY, USA, ²US Geological Survey, Woods Hole, Massachusetts, USA, ³Icelandic Meteorological Office, Reykjavik, Iceland

Contents of this file

Text S1 to S2
Figure S1 to S13

Introduction

The supporting information includes a short discussion regarding the water current velocity measurements made on along the Mid-Atlantic Bight (MAB) onboard the R/V Hugh R. Sharp from Aug 25 – Sept 5, 2017. The discussion focuses on relating CH₄ concentration measurements to the presence of nearby gas seeps while taking into account water current direction. Furthermore, we discuss the limitations of these measurements and important caveats regarding this type of analysis. The first two figures of the supporting information compares water current direction and velocity between two sampling transects, the first figure showing data from the surface to 100 m depth and the second showing data from 200 – 400 m. The third figure shows a plot of density against depth for the deepest stations from transects 1-5. Figures S4 – S7 show interpolated CH₄ concentration and stable isotopic values for all transects that were not presented in the main text . Figures S8 – S13 show temperature, salinity and density plots based on measurements using a SeaBird Electronics 911 plus CTD. Each plot shows the temperature, salinity and density for a different transect.

Text S1. Water Current Velocity and Direction

For most stations, water current velocities were greatest near the surface and decreased with depth. One notable exception are the stations at transect 2, where current velocities were relatively low near the surface and increased to a maximum at depths of 150 - 200 m, depending on the station. Water current direction varied with depth at all stations, however, water current direction was consistent among stations within a transect when considering similar depths. For example, water currents show a similar pattern among the stations at transect 4, since currents moved towards the southeast near the surface, shifted towards the north at 200 - 400 m depth, then veered towards the west and south at greater depths. On the other hand, water current direction at transect 2 was not very consistent among stations. Near the surface, currents moved towards the east, south, and west, and at greater depths such variability in water current direction persisted among stations at transect 2. Figure S1 and S2 show rose diagrams of water current velocity and direction for transect 2 and 4 from the surface to 100 m depth and from 200 – 400 m depth, respectively.

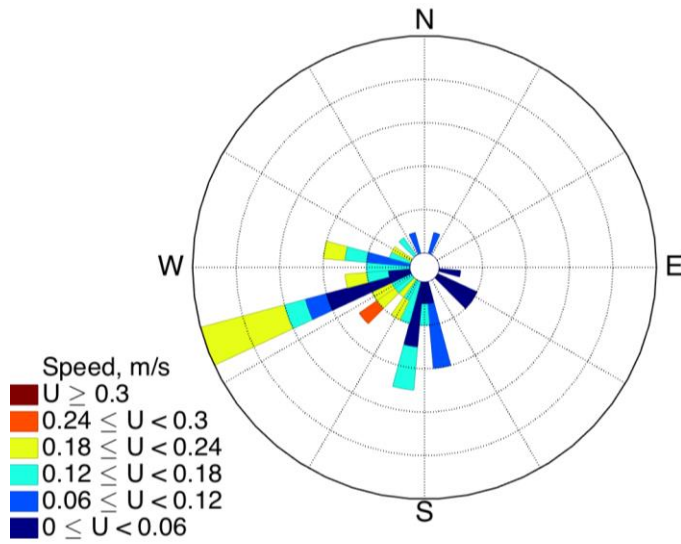
Text S2. Methane Transport

Water circulation plays an important role in controlling the spatial distribution and magnitude of CH₄ concentrations in the water column (Mau et al., 2012). Near the seafloor where gas seeps are present, water currents are responsible for transporting CH₄ away from the seep source. Water circulation also leads to a reduction in CH₄ levels due to mixing between high CH₄ concentration and low CH₄ concentration waters. Based on water current direction estimates, we investigated whether elevated CH₄ concentrations could be correlated to the gas seeps we identified on this cruise as well as previously published locations of gas seeps (Skarke et al., 2014). For example, two clusters of gas seeps have been identified just to the south of transect 2. The gas seeps within these clusters originate at depths of 280 – 315 m and 422 - 484 m, which is similar to the depths where elevated CH₄ concentrations were measured at several stations from transect 2, 275 – 300 m and 400 m. The direction of water currents at transect 2 differed among stations at these depths. However, for certain stations at transect 2, water currents moved towards the north and northwest making it possible for these seeps to influence the CH₄ concentrations measured at transect 2. On the other hand, it is not clear which seeps were responsible for the high CH₄ concentrations measured at transect 3. The highest CH₄ concentrations at transect 3 were measured at 400 – 450 m depth and while a large cluster of seeps was found between transect 3, station 1 and transect 3, station 3, the deepest seep originated at a depth of 388 m. Furthermore, these high CH₄ concentrations were measured at transect 3, stations 4 and 5, which lie to the east of the other stations in this transect, yet water currents were moving towards the west at these depths. Near transect 4, we observed the potential for seep CH₄ transport, but this was not necessarily reflected in our CH₄ concentration measurements. Just south of transect 4, a cluster of seeps has been identified originating at depths of 211 – 494 m. For most stations at transect 4 at depths between 200 – 400 m, water currents were moving consistently towards the north (Figure S2), yet CH₄ concentrations measured at these

depths were not much greater than background. It could be that the seeps identified south of transect 4 are ephemeral in their emission of CH₄ or the CH₄ flux from these seeps is quite low. It is also possible that over longer timescales water currents at this location were not necessarily moving to the north as shown by the limited view of our LADCP measurements.

The associations between CH₄ concentrations, gas seep locations, and water current direction discussed above were straightforward for certain stations but not for others, likely due to several limitations. First, the presence and location of gas seeps along the MAB is still a topic of active research, and for the seeps that have been identified, it is not clear the extent to which their emissions are transitory. The data collected on this cruise confirms the location of certain seeps published by Skarke et al. (2014), but also shows a number of gas seeps that have not been published previously. For the seeps that have been identified, it is not clear how much CH₄ they inject into the water column and thus what potential they have to increase dissolved CH₄ concentrations. Furthermore, the LADCP measurements simply provide a snapshot of the water circulation patterns at the time and location where water samples were collected. This adds some uncertainty when correlating high CH₄ concentration measurements to specific gas seep locations, since the direction of water currents could change over different timescales.

A - Transect 2



B - Transect 4

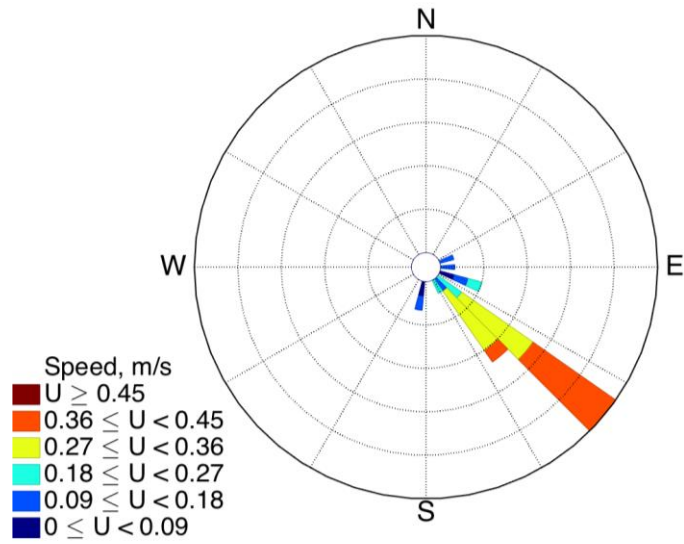
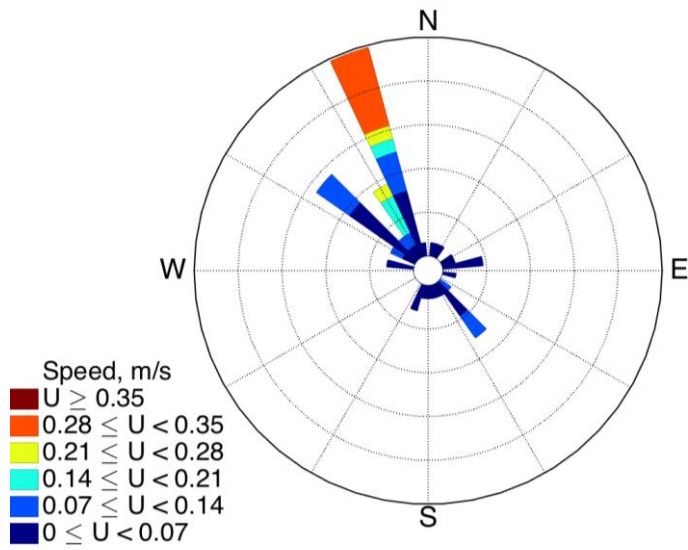


Figure S1. Rose diagrams of water current velocities and direction from the surface to 100 m depths at transects 2 and 4. Current speed (m/s) is color coded based on its magnitude.

A - Transect 2



B - Transect 4

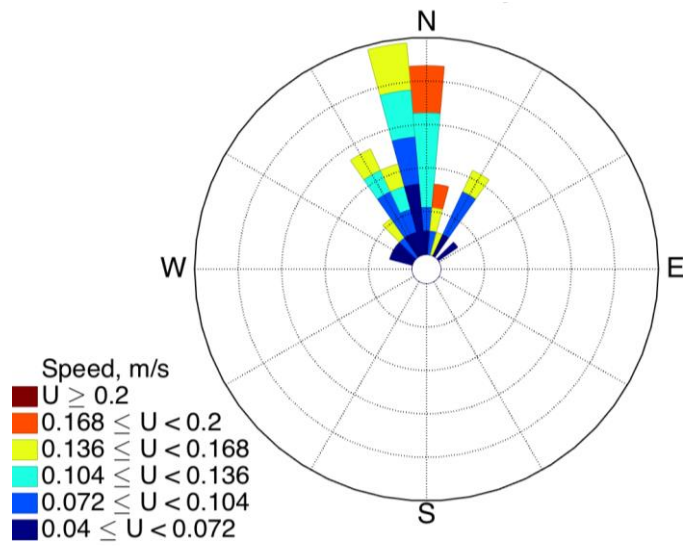


Figure S2. Rose diagrams of water current velocities and direction from the 200 - 400 m depths at transects 2 and 4. Current speed (m/s) is color coded based on its magnitude.

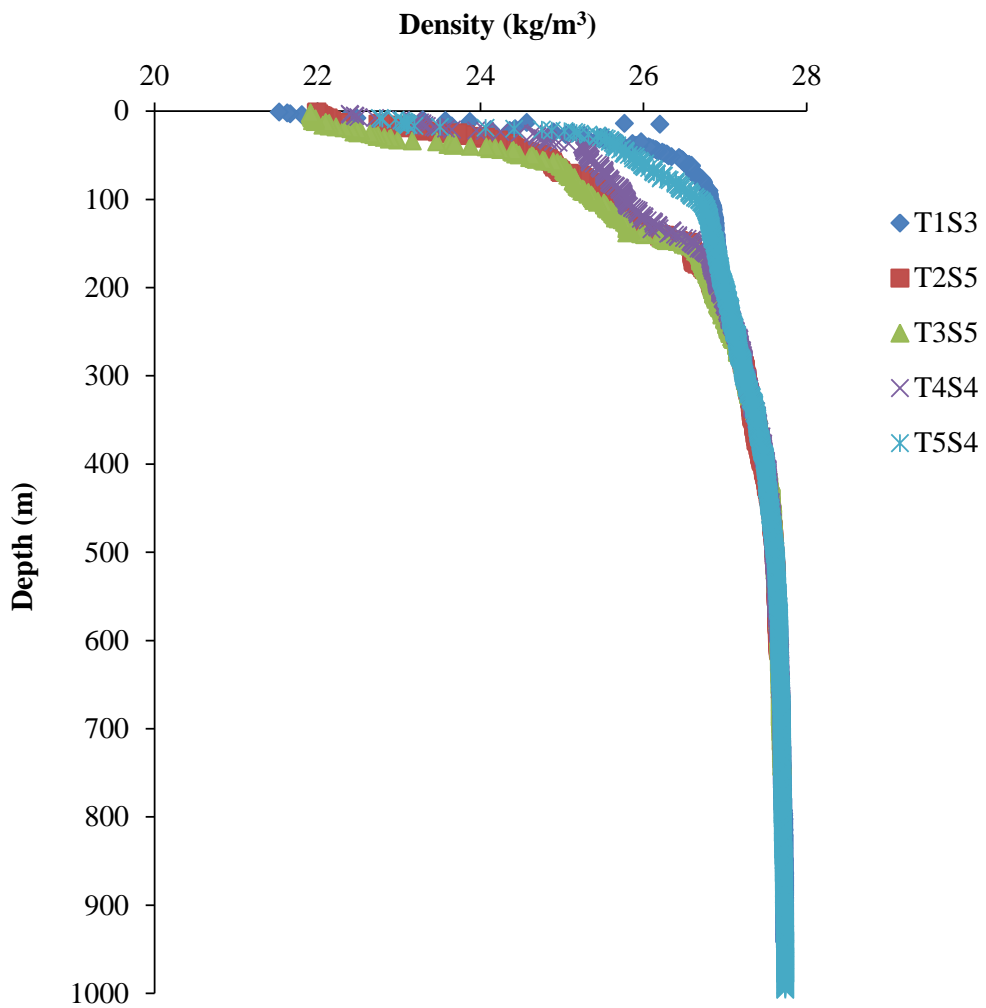


Figure S3. Plot of density against depth for several stations along the MAB. Data from the stations with the greatest depth from transects 1-5 are shown. In the deeper part of the water column, below 200 m, the relationship between density and depth is consistent among all stations plotted.

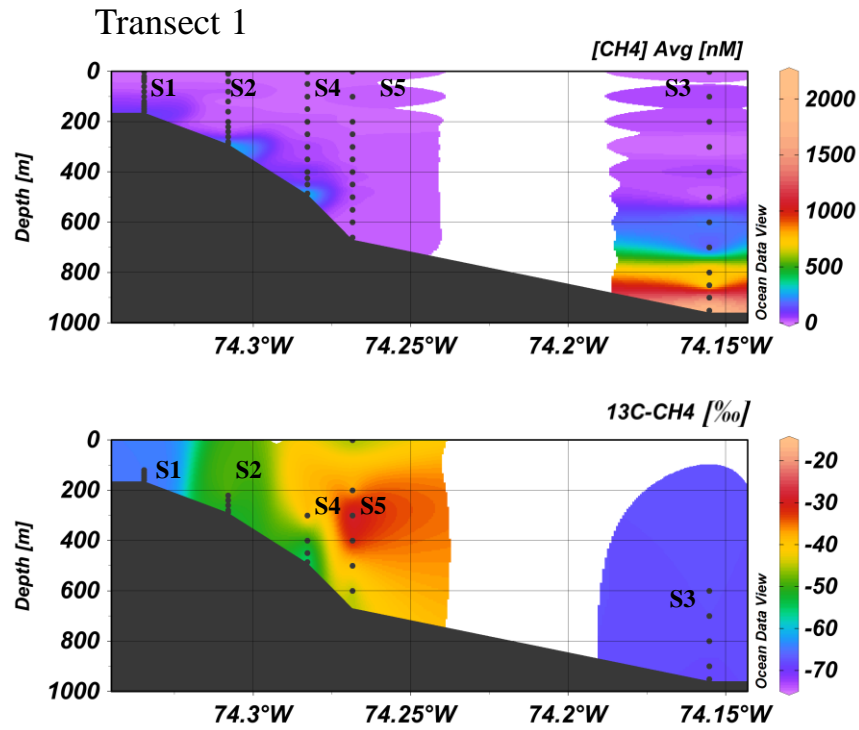


Figure S4. Interpolated CH₄ concentration and $\delta^{13}\text{C}\text{-CH}_4$ measurements for transect 1. Black dots show where specific water samples were collected. Measured data was interpolated using Ocean Data View.

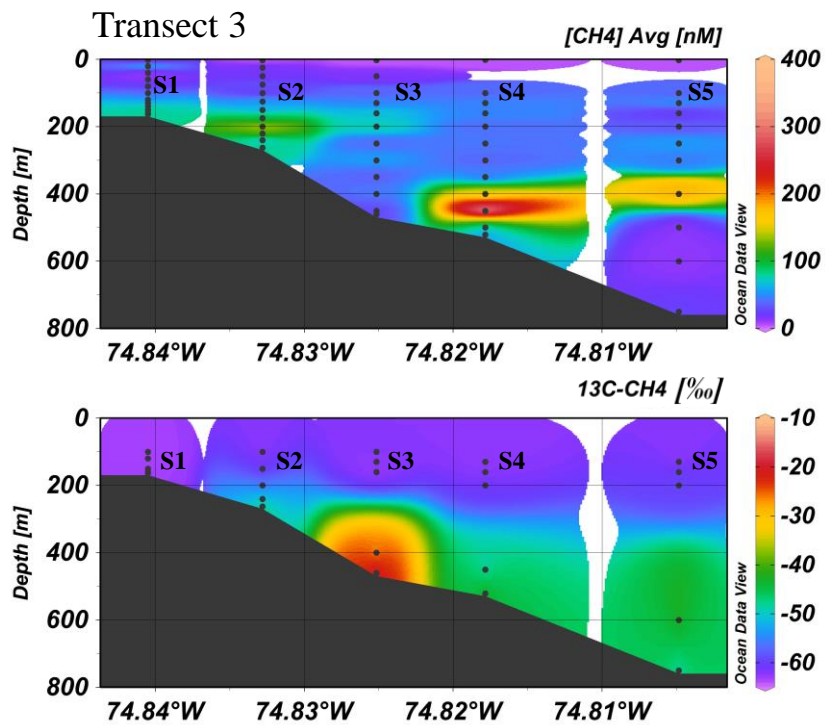


Figure S5. Interpolated CH₄ concentration and δ¹³C-CH₄ measurements for transect 3. Black dots show where specific water samples were collected. Measured data was interpolated using Ocean Data View.

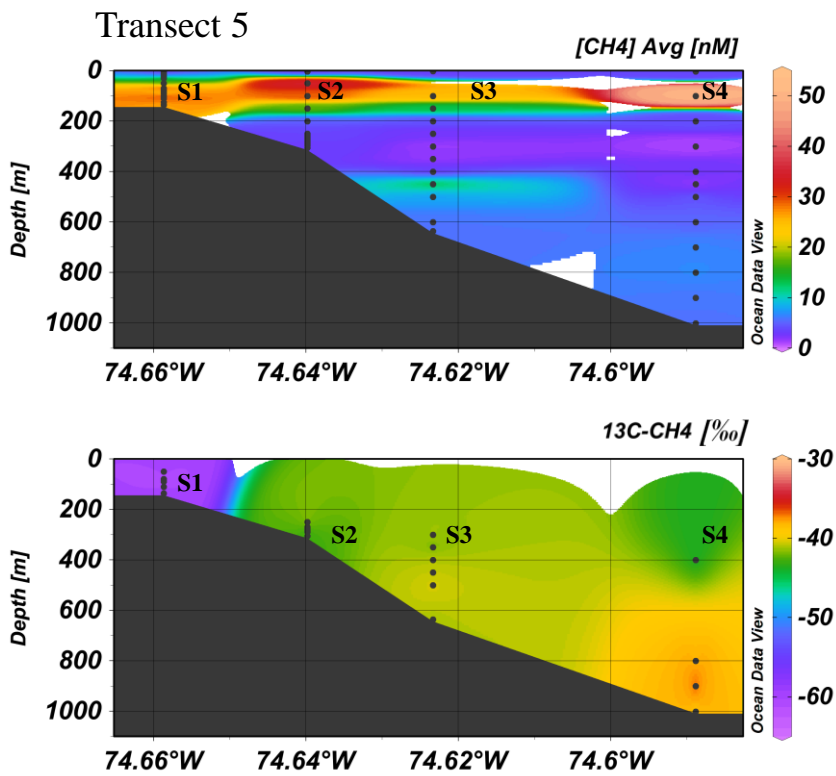


Figure S6. Interpolated CH₄ concentration and δ¹³C-CH₄ measurements for transect 5. Black dots show where specific water samples were collected. Measured data was interpolated using Ocean Data View.

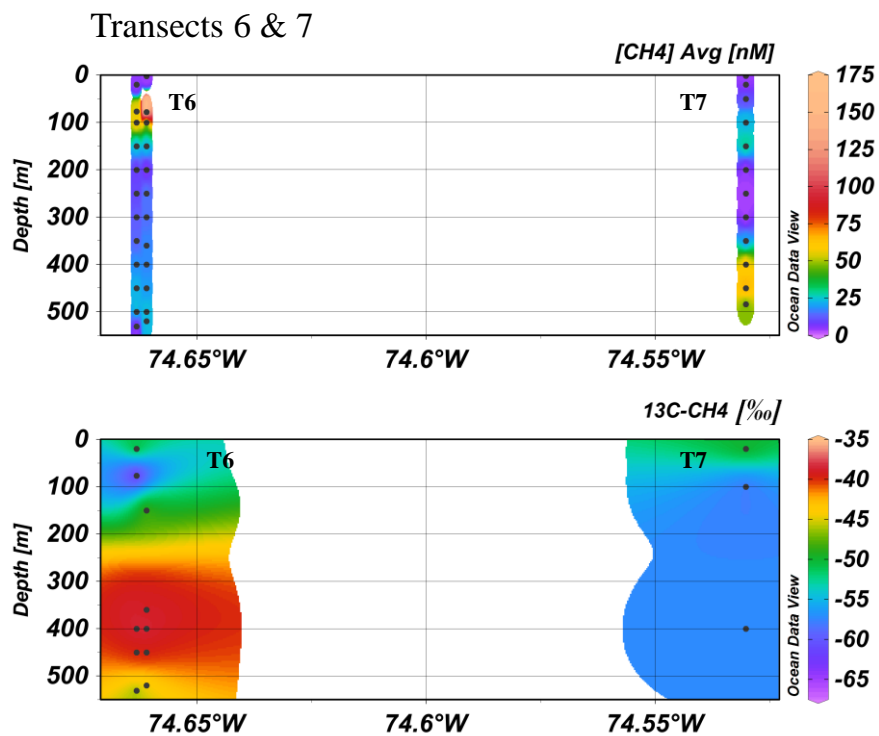


Figure S7. Interpolated CH₄ concentration and δ¹³C-CH₄ measurements for transects 6&7. Black dots show where specific water samples were collected. Measured data was interpolated using Ocean Data View.

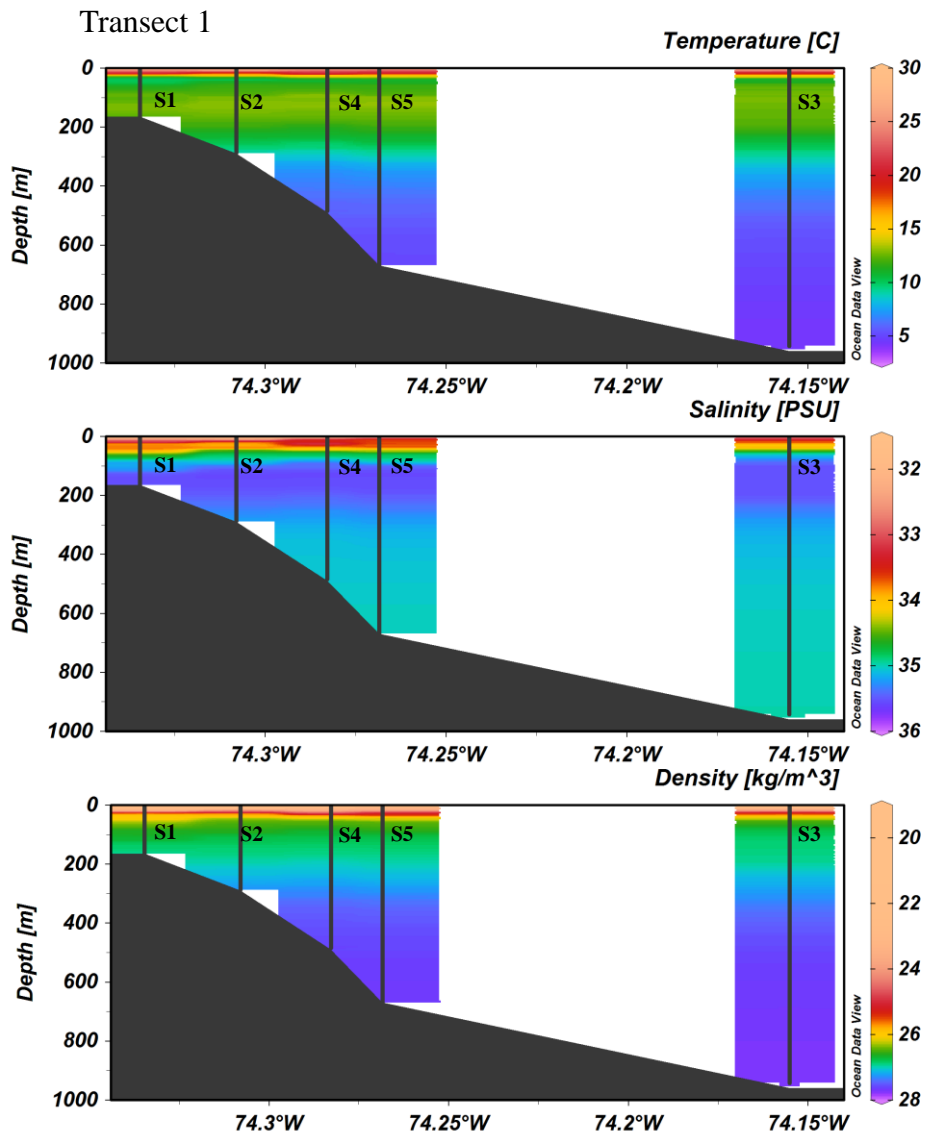


Figure S8. Plots of temperature (°C), salinity (PSU) and density (kg/m³) measured for transect 1. Black lines show where data was measured by the CTD at each station. Measured data was interpolated using Ocean Data View.

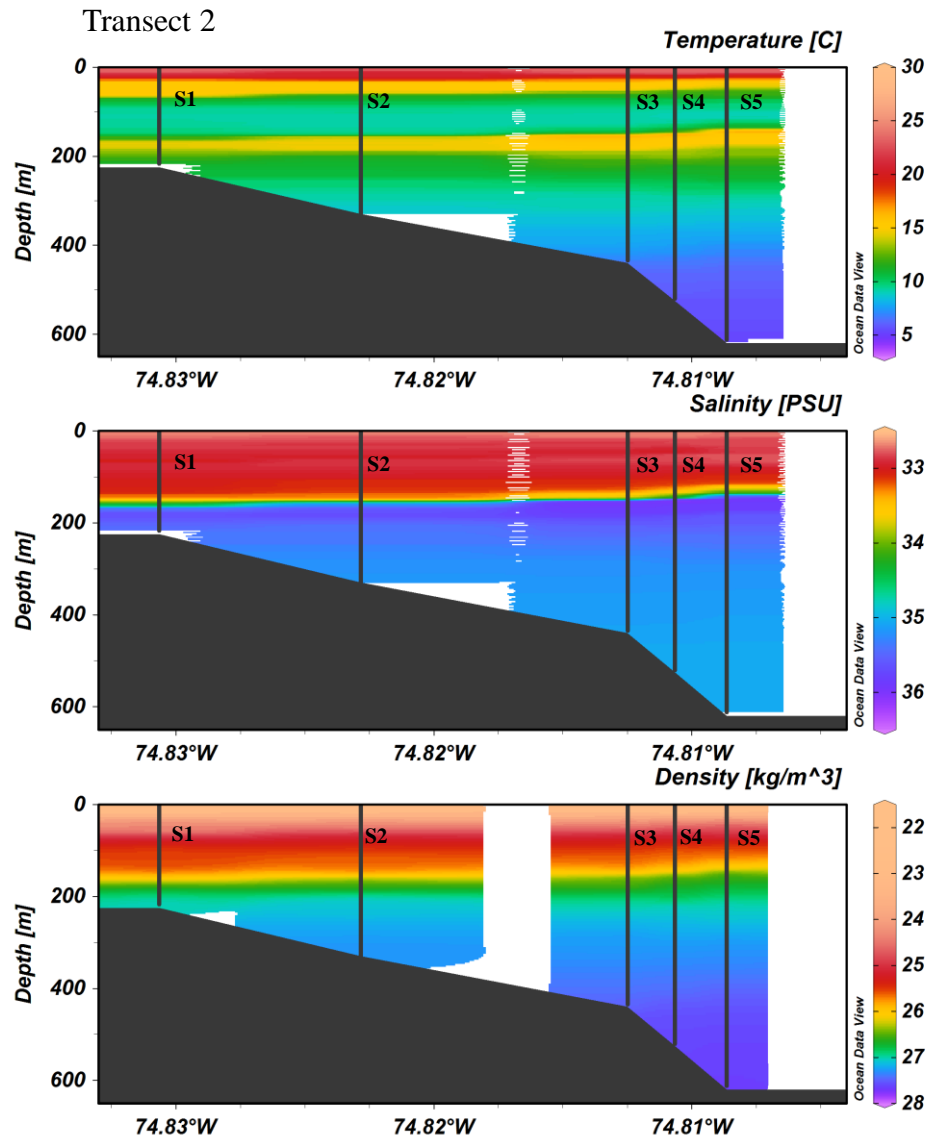


Figure S9. Plots of temperature (°C), salinity (PSU) and density (kg/m³) measured for transect 2. Black lines show where data was measured by the CTD at each station. Measured data was interpolated using Ocean Data View.

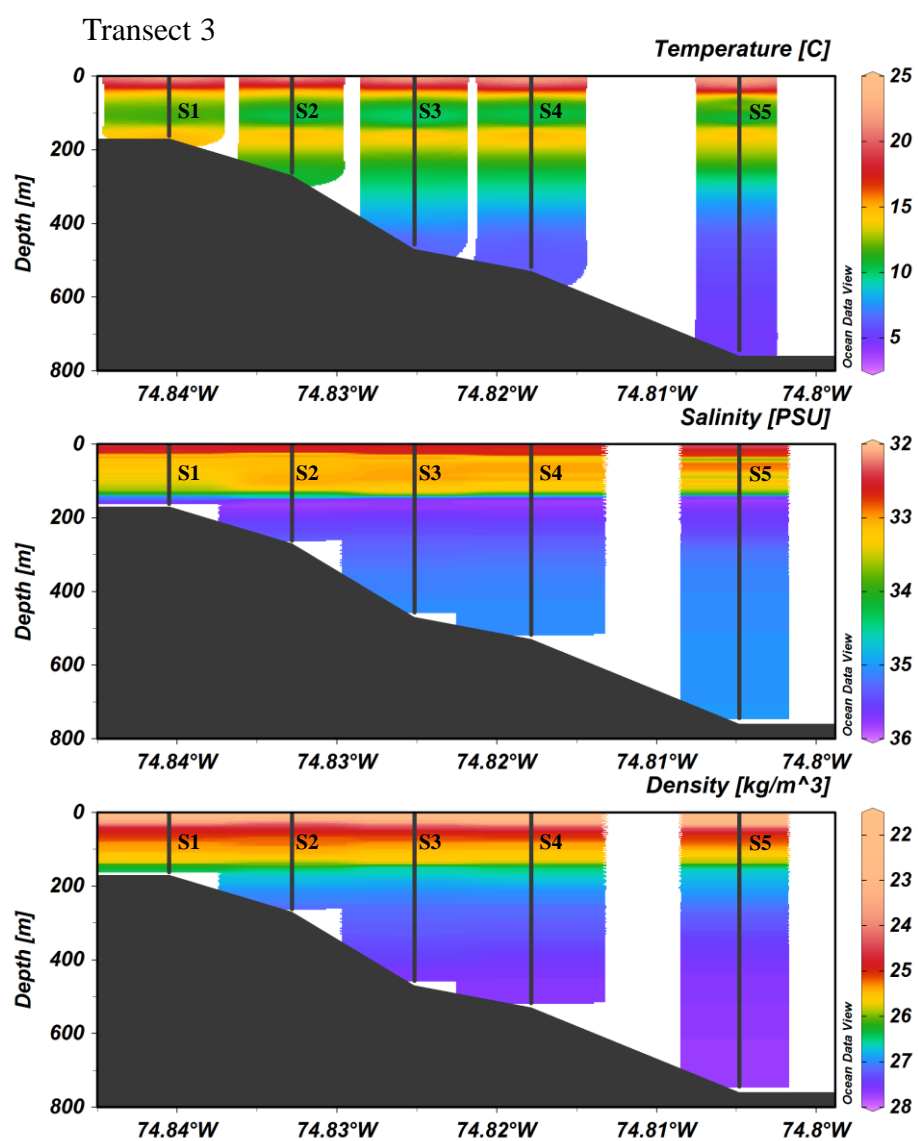


Figure S10. Plots of temperature (°C), salinity (PSU) and density (kg/m³) measured for transect 3. Black lines show where data was measured by the CTD at each station. Measured data was interpolated using Ocean Data View.

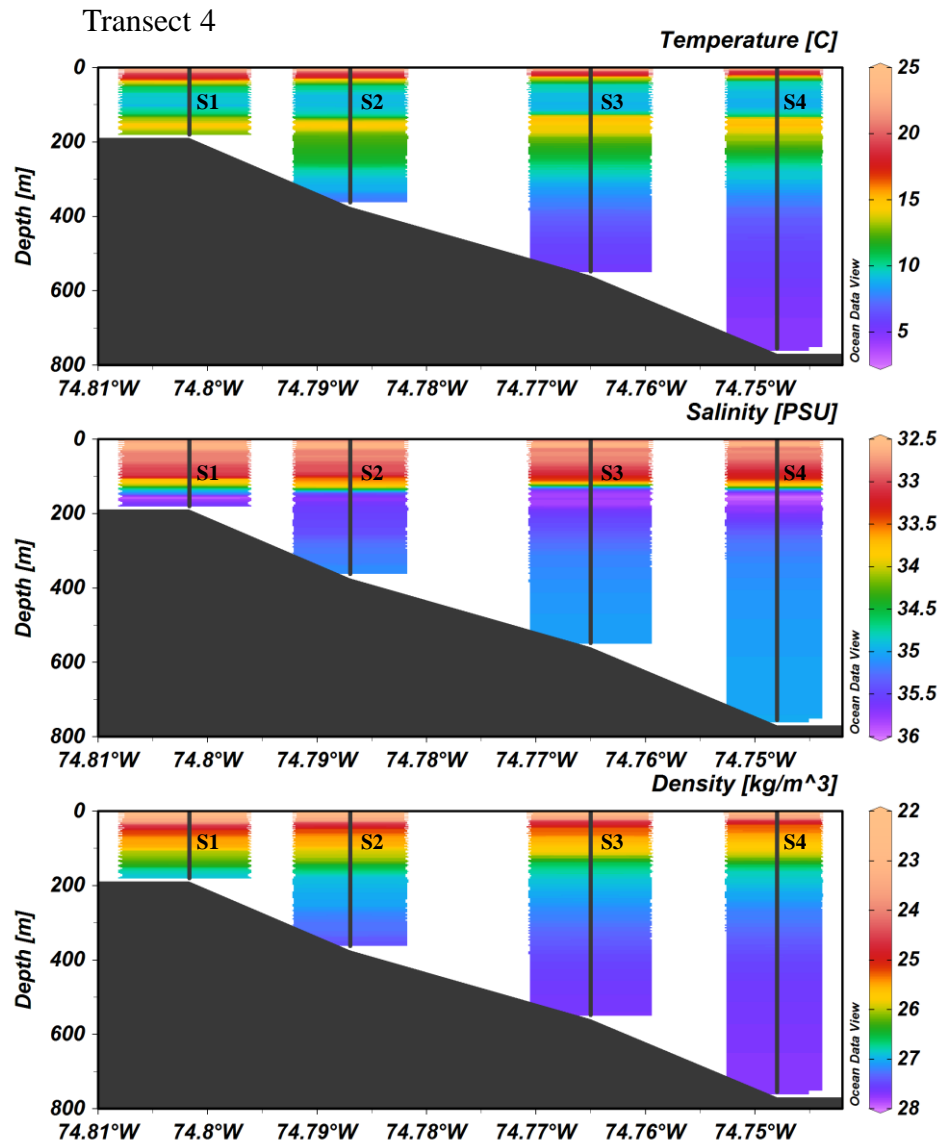


Figure S11. Plots of temperature (°C), salinity (PSU) and density (kg/m³) measured for transect 4. Black lines show where data was measured by the CTD at each station. Measured data was interpolated using Ocean Data View.

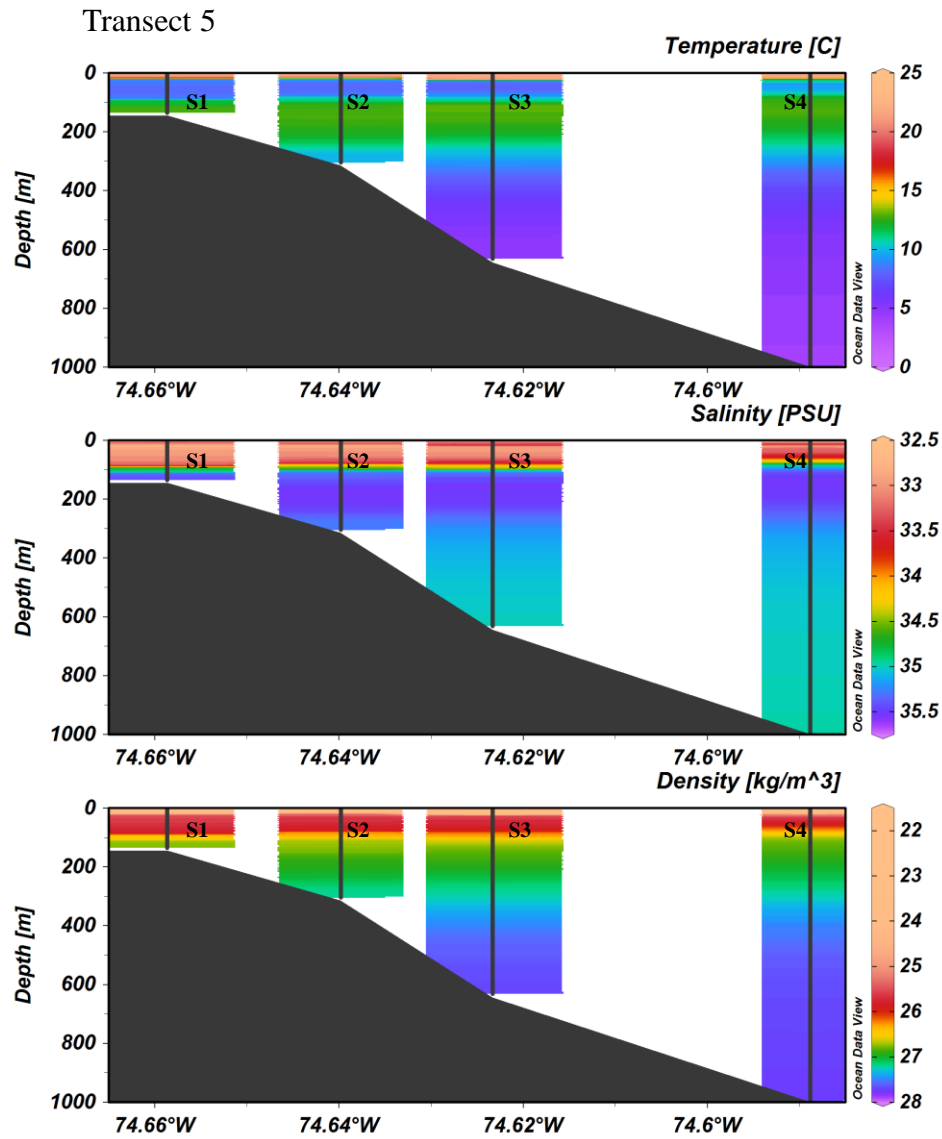


Figure S12. Plots of temperature (°C), salinity (PSU) and density (kg/m³) measured for transect 5. Black lines show where data was measured by the CTD at each station. Measured data was interpolated using Ocean Data View.

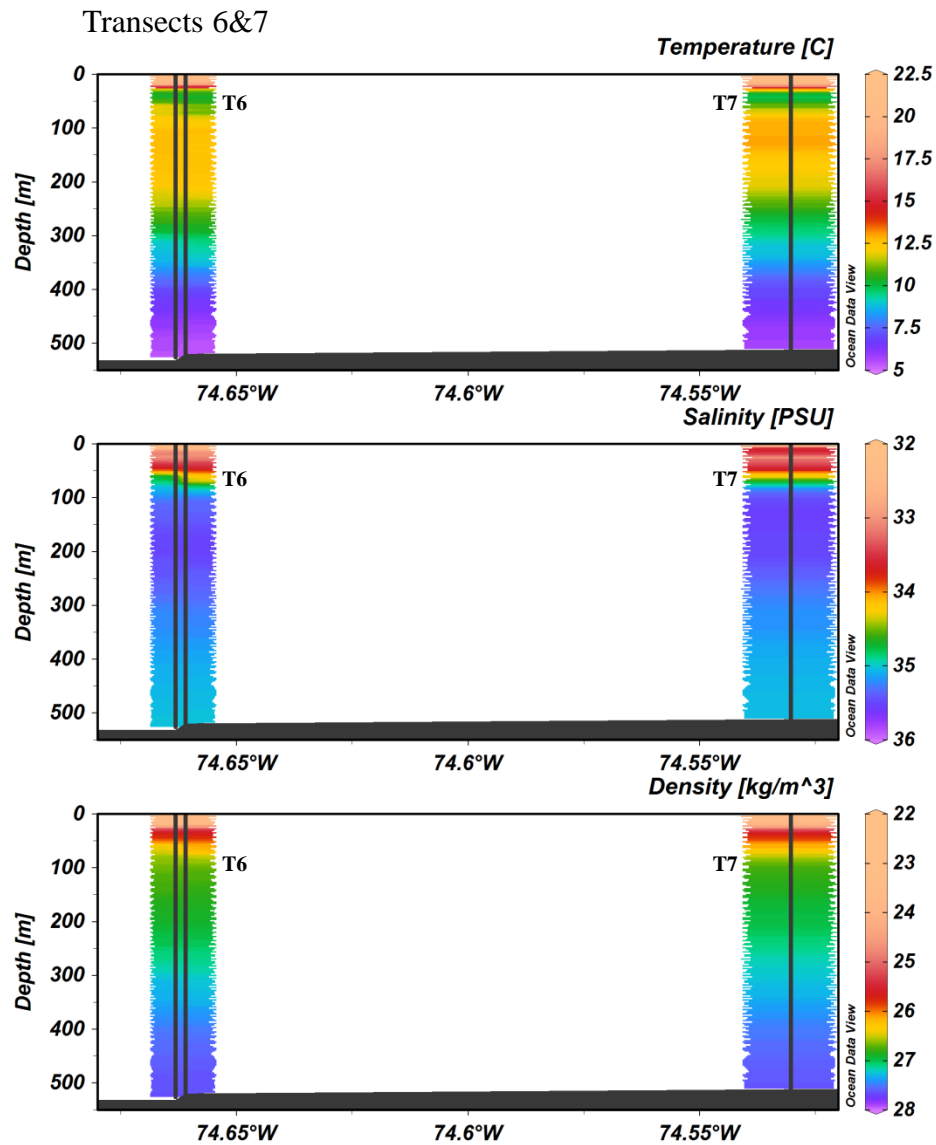


Figure S13. Plots of temperature ($^{\circ}\text{C}$), salinity (PSU) and density (kg/m^3) measured for transects 6 and 7. Black lines show where data was measured by the CTD at each station. Measured data was interpolated using Ocean Data View.

References

- Mau, S., Heintz, M. B., & Valentine, D. L. (2012). Quantification of CH₄ loss and transport in dissolved plumes of the Santa Barbara Channel, California. *Continental Shelf Research*, 32(0), 110–120. <https://doi.org/http://dx.doi.org/10.1016/j.csr.2011.10.016>
- Skarke, A., Ruppel, C., Kodis, M., Brothers, D., & Lobecker, E. (2014). Widespread methane leakage from the sea floor on the northern US Atlantic margin. *Nature Geoscience*, 7(9), 657–661. <https://doi.org/10.1038/ngeo2232>